Chemical Treatment of Banana Blossom Peels Adsorbent as New Approach for Manganese Removal: Isotherm and Kinetic Studies

Nurul Nadia Rudi
Universiti Tun Hussein Onn Malaysia
Najeeha Mohd Apandi
Universiti Tun Hussein Onn Malaysia
Mimi Suliza (msuliza@uthm.edu.my)
Universiti Tun Hussein Onn Malaysia https://orcid.org/0000-0003-0609-8486
Suhair Omar
Universiti Tun Hussein Onn Malaysia
Norshuhaila Mohamed Sunar
Universiti Tun Hussein Onn Malaysia
Lee Te Chuan
Universiti Tun Hussein Onn Malaysia
Ramathasan Nagarajah
Universiti Tun Hussein Onn Malaysia

Research Article

Keywords: Banana blossom peels, Manganese, Adsorption isotherm, Kinetic study, Desorption

Posted Date: February 23rd, 2022

DOI: https://doi.org/10.21203/rs.3.rs-1319392/v1

Chemical Treatment of Banana Blossom Peels Adsorbent as New Approach for Manganese Removal: Isotherm and Kinetic Studies

Nurul Nadia Rudi[1], Najeeha Mohd Apandi[2], Mimi Suliza Muhamad[2*], Suhair Omar[1], Norshuhaila Mohamed Sunar[1], Lee Te Chuan[3], Ramathasan Nagarajah[1]

[1] Department of Civil Engineering Technology, Faculty of Civil Engineering Technology, Universiti Tun Hussein Onn Malaysia, Pagoh Education Hub, 84600 Pagoh, Muar, Johor, Malaysia

[2]Sustainable Engineering Technology Research Centre (SETechRC), Faculty of Engineering Technology, Universiti Tun Hussein Onn Malaysia, Pagoh Education Hub, 84600 Pagoh, Muar, Johor, Malaysia

[3] Department of Production and Operation Management, Faculty of Technology Management and Business, Universiti Tun Hussein Onn Malaysia, 86400 Parit Raja, Batu Pahat, Johor, Malaysia

***Corresponding author:**
Mimi Suliza Muhamad
E-mail: msuliza@uthm.edu.my

ABSTRACT

The current study determined the potential of chemical modified banana blossom peels (BBP) as an adsorbent for the removal of manganese (Mn) from water. The BBP adsorbent was characterized using Field Emission Scanning Electron Microscopy (FESEM), Fourier Transform Infrared Spectroscopy (FTIR), X-Ray Diffraction (XRD) and Brunauer-Emmet Teller (BET). The effects of the solution pH, adsorbent dosage, initial manganese concentration and contact time towards the adsorption process were evaluated in batch adsorption studies. FESEM analysis displayed a deeper dents and rough internal surface that cater for deposition of Mn, while EDX analysis detected the presence of C, O, and Na elements (before adsorption); C, O and Mn (after adsorption). FTIR analysis revealed presence hydroxyl, carboxylic and amino groups which are responsible for the adsorption process. Moreover, XRD analysis showed that the structure of the BBP adsorbent is amorphous. The BET surface area of BBP adsorbent was 2.12 m^2/g with the total pore volume of 0.0139 cm^3/g and average pore diameter of 64.35 nm. The BBP adsorbent showed promising results of 98% Mn removal at optimum condition of pH 7, 0.5 g (adsorbent dosage), 10 mg/L of Mn initial concentration in 150 min contact time. Adsorption isotherm data were fitted with linear Langmuir and linear Freundlich model best fit with $R^2 > 0.98$, while the adsorption process take place as a function of chemisorption process as determined using linear pseudo-second order kinetics. The maximum desorption rate of Mn was achieved at 92% in the first cycle with recovery rate of 94.18% Mn removal within 30 min using 0.1 M HCl. These findings confirmed the potential BBP as a natural adsorbent for Mn removal as an effective treatment option for enhancing wastewater quality.

Keywords: Banana blossom peels, Manganese, Adsorption isotherm, Kinetic study, Desorption

Statements and Declarations

Ethics approval and consent to participate

All procedures performed in the present study involving human participants were in accordance with the ethical standards of the institutional and/or national research committee.

Consent for publication

Not applicable

Availability of data and materials

The authors confirm that the data supporting the findings of this study are available within the article. The lead author* affirms that this manuscript is an honest, accurate, and transparent account of the study being reported; that no important aspects of the study have been committed; and that any discrepancies from the study as planned and have been explained.

Competing Interests

The authors declare that they have no competing interests.

Funding

This study was funded by the Ministry of Higher Education (MOHE), Malaysia under the Fundamental Research Grant Scheme grant (K219) (FRGS/1/2019/TK10/UTHM/03/3).

Authors contributions

All authors contributed to the study conception and design. Conceptualization: Mimi Suliza Muhamad; Methodology: Mimi Suliza Muhamad; Norshuhaila Mohamed Sunar; Material preparation, data collection, and analysis: Nurul Nadia Rudi; Najeeha Mohd Apandi; Ramathasan Nagarajah, Writing – original draft preparation: Nurul Nadia Rudi; Review and editing: Najeeha Mohd Apandi; Mimi Suliza Muhamad, Ramathasan Nagarajah; Funding acquisition: Mimi Suliza Muhamad, Resources: Suhair Omar; Lee Te Chuan, Supervision: Mimi Suliza Muhamad; The first draft of the manuscript was written by Nurul Nadia Rudi and all authors commented on previous versions of the manuscript. All authors read and approved the final manuscript.

64 **Acknowledgement**

65 The authors thank the parties involved in this project, especially Universiti Tun Hussein Onn Malaysia, for
66 providing the research facilities and equipment. The authors wish to thank the Ministry of Higher Education
67 Malaysia for the Fundamental Research Grant Scheme grant (K219) (FRGS/1/2019/TK10/UTHM/03/3).

68 **Conflict of Interest Statement**

69 We declare that this manuscript is original, has not been published before and is not currently being considered
70 for publication elsewhere. We have no conflicts of interest to disclose with this publication. We have no known
71 competing financial interests or personal relationships that could have appeared to influence the work reported in
72 this paper.

1. INTRODUCTION

The rapid industrial development has increased water sources pollution (Ahmed et al. 2014). Disposal of contaminants that include toxic sludge, solvents, and heavy metals from industrial activities into water bodies had been reported to be 300–400 million tonnes annually (Singh et al. 2018). The number of polluted water sources in Malaysia increases over time due to the uncontrollable waste disposal and effluent discharge from industry (Marsidi et al. 2018). The waterworks company had alarmed the presence of heavy metals detected in river due to discharged from industrial effluents (Zou et al. 2016). In steel production, manganese (Mn) had been widely used and discharged in the industrial effluents. Mn is a trace metal that is found mainly as oxides, carbonates, and silicates in many different minerals, with pyrolusite (manganese dioxide) as the most common naturally-occurring form (Milatovic and Gupta, 2018). Mn can be found abundantly in the earth's crust and water sources, which exist in a broad range of oxidation states and species in the water (Tobiason *et al.*, 2016)

Upon oxidation, Mn becomes insoluble in water and change the colour of the water into brown-red colour, making the water aesthetically unpleasant and unfit for drinking (Marsidi et al. 2018; Bouchard et al. 2018; Ali et al. 2017; Rumsby et al. 2018). Studies have shown consumption of high Mn concentration in drinking water led to adverse health effects related to neurological disorders, intellectual, and cognitive development (Rumsby et al. 2018; Gerke et al. 2016). Accumulation of excessive Mn ions in specific brain areas can cause neurotoxicity and degenerative brain disorder (Idrees et al. 2018; Milatovic and Gupta, 2018). Exposure of 240-350 µg/L Mn ions concentration toward children displayed symptoms of reduced manual dexterity, speed, short-term memory, and visual recognition (Mthombeni et al. 2016).

Various treatment technologies have been used to treat water containing manganese including ion exchange, oxidation, chemical precipitation, electrochemical treatment, ozone, membrane filtration, and ultraviolet irradiation (Baysal et al. 2013; Carolin et al. 2017; Al-Jubouri and Holmes, 2013; Du et al. 2019; Alvarez-Bastida et al. 2018; Jeirani et al. 2015; Fatemeh et al. 2018; Ihsanullah et al. 2016; Ahmadi et al. 2019). Most of the technologies are able to remove Mn in water, however there are some problems arise such as complex process, space requirements, treatment capacity, sludge disposal, high operational and maintenance cost (Marsidi et al. 2018; Ali 2017; Jawed and Pandey 2019). Among the treatment technologies, adsorption process has been known to be effective in removing contaminants with minimal problem. Agricultural waste adsorbent particularly has gaining attention among researchers in treating water containing Mn ions owing to its efficiency, availability, environmental friendly, and easy to produce (Jawed and Pandey. 2019). Agricultural waste are found abundantly

in Malaysia and can be utilize to produce low-cost adsorbents. Banana plant particularly is widely planted and used for many purposes. About 16% of the total fruit production encompass of banana making it the second largest fruit produced worldwide with the highest of 32% produced fruit in Malaysia (Pathak et al. 2017).

Currently, the study on banana blossom as adsorbent for the removal of contaminant is limited. Gopakumar et al. (2018) studied on banana blossom peels adsorbent by simply washing and drying the peels under sunlight. The banana blossom peels (BBP) adsorbent is able to remove 79.72% turbidity, 88.24% total solids, and 61.01% chloride in lake water sample as well as reducing the alkalinity of the water to neutral pH (8.4 to 6.75). Herawati et al. (2018) used BBP adsorbent to treat dyes that able to removed Congo Red dye (1.78%), Remazol Yellow dye (4.29%), Methylene Blue dye (0.43%), and Remazol Black dye (0.56%). Yet, chemical treatment of BBP as an adsorbent for Mn removal has not been investigated before.

According to our knowledge, no study was performed on the isotherm and kinetic studies towards the reusability and application of the chemical modified BBP adsorbent for Mn removal. Therefore, the present study attempts to synthesize banana blossom peels (BBP) via chemical treatment method. The adsorption behaviour of the Mn onto the BBP adsorbent was investigated in terms of different factors that influence the process including pH, adsorbent dosage, initial manganese concentration and contact time. The adsorption mechanism analysis was elucidated by isotherm and kinetic studies to determine the mechanism of the adsorption process.

2. MATERIALS AND METHODS

2.1. Preparation of Banana Blossom Peels Adsorbent

Banana blossom peels (BBP) were obtained from the banana planters located in Pagoh Jaya, Muar, Johor, Malaysia. BBP was cleansed and washed thoroughly to remove impurities on the surface; then the BBP was then cut into small pieces' oven dried at 60ºC ± 1 ºC for 12 hrs. The BBP were grounded and sieved into powder with standard mesh ring of 150-212 µm. The obtained BBP powder was immersed in 20 ml of 1 M HCl and sodium hydroxide (NaOH). The BBP powder with chemical activation solutions were stirred in an orbital shaker at 150 rpm for 30 min. The BBP was then rinsed with distilled water to eliminate any remaining chemical on the surface. The BBP powder is next dried in an oven at 60ºC ± 1 ºC for 12 hrs (Surovka and Pertile 2017) until it dry and sieve using standard 60 mesh sieve. The schematic representation of BBP adsorbent preparation is shown in Figure 1.

2.2. Characterization of Banana Blossom Peels Powder

Field emission scanning electron microscope (FESEM) and Energy Dipersive X-ray (EDX) were used to determine the surface morphology and elemental composition of BBP adsorbent. The functional groups in BBP

adsorbent were analysed using a Fourier transform infrared spectroscopy (FTIR). The FTIR spectrum was conducted at resolution of 4 cm^{-1} and the reading was recorded at mid-infrared of region 4000 to 400 cm^{-1}. X-ray Diffraction (XRD) pattern using Bruker D8 Advanced was utilized to determine the crystalline structure of the BBP pattern using Bruker D8 Advanced. X-rays of 1.5406 Å wavelength was generated by Cu Kα monochromatic radiation. The BBP adsorbent was compressed in a cassette sample holder and the data was collected from 2θ = 20° - 80° with sampling pitch of 0.02°.

The surface area, total pore volume, and pore diameter were measured by a Brunauer-Emmett-Teller (BET) method based on nitrogen adsorption-desorption at 77K (Thermo Scientific surface area and pore analyser). Prior to analyses, the BBP adsorbent sample was outgassed at 60 ^{o}C for 24 hrs.

2.3. Batch Adsorption Experiment

Batch adsorption experiments were conducted in 250 mL conical flask shaken by using Stuart orbital shaker at 150 rpm with different pH (4-9), adsorbent dosage (0.1-0.7 g/L), initial Mn^{2+} concentrations (10-50 mg/L) and contact time (60-180 minutes). A stock solution with Mn concentration of 100 mg/L was prepared by dissolving 0.308 g of manganese (II) sulphate in one L deionized water. The experimental solutions were further diluted to different concentrations of 10 - 50 mg/L in 1 L flasks. The Mn removal efficiency (%) and adsorption capacity, q_e (mg/g) were determined as follows:

$$\text{Removal (\%)} = \frac{(C_o - C_e)}{C_o} \times 100 \quad (1)$$

$$q_e = \frac{V\,(C_o - C_e)}{W} \quad (2)$$

where:

C_o (mg/l): Initial Mn concentration

C_e (mg/l): Equilibrium Mn concentration in solution

q_e (mg/g): The amount of metal ions

V: The solution volume (L)

W: The mass of BBP adsorbent (g).

The suspension of the samples was filtered with 0.45 μm filter paper prior and analyzed for Mn concentration using inductively coupled plasma optical emission spectrometry (ICP-OES) (Perkin Elmer, Optima 8000). This technique was to measure the concentration of Mn before and after the adsorption batch experiments procedure.

2.4. Adsorption Isotherms Studies

The adsorption isotherms are important in order to demonstrate the behaviour, mechanism and the optimum fitting through metal ions concentration in the liquid state in the surface of adsorbents at a given concentration (Mahmoud et al, 2014). In this study, the adsorption isotherm was analyzed by Langmuir and Freundlich model to find out the relationship between the Mn^{2+} concentration adsorbed by BBP according to the linear and non-linear equations.

The Langmuir isotherm was assumed as monolayer adsorption of solutes onto an adsorbent surface. The Langmuir isotherm equation is written as:

Linear:

$$\frac{C_e}{q_e} = \frac{1}{q_{max}b} + \frac{C_e}{q_{max}} \quad (3)$$

Non-Linear:

$$q_e = \frac{q_{max} \pm bC_e}{(1+bC_e)} \quad (4)$$

where C_e is the equilibrium concentration of solute and q_{max} is monolayer capacity of the adsorbent (mg/g), and b is the adsorption constant (L/mg). The plot of C_e/q_e versus C_e should be a straight line (Adekola et al. 2014).

The Freundlich isotherm is more commonly known relationship to describe the non-ideal and reversible adsorption. The Freundlich isotherm is presented by the following equation:

Linear:

$$\log q_e = \log K_F + \frac{1}{n}\log C_e \quad (5)$$

Non-linear:

$$q_e = K_f + {C_e}^{1/n} \quad (6)$$

Where Kf is the Freundlich constants denoting the adsorption capacity (mg/L), qe is the uptake of pollutant per unit weight of biosorption (mg/L), Ce is the equilibrium of concentration (mg/L), and n is the empirical constant indicating of adsorption intensity

2.5. Adsorption kinetics studies

The Mn removal data obtained from the experiment under optimal conditions were applied to linear and non-linear models of pseudo first and second order kinetics to generate the prediction adsorption data. The reaction rate and mechanism of adsorption process can be determined from kinetic study. The pseudo-first order assumes that the uptake rate of Mn ions with time is directly proportional to the number of unoccupied sites on the BBP adsorbent (Fathi et al. 2020). The pseudo-first order equation which represented the adsorption of a solute from a liquid solution is written as below:

Linear:

$$\ln(q_e - q_t) = \ln q_e - K_1 t \quad (7)$$

Non-linear:

$$q_t = q_e (1 - e^{-K1t}) \quad (8)$$

Where q_e is the adsorbed metal ion mass at equilibrium (mg/g), q_t is the adsorbed metal ion mass at time t (mg/g), K_1 is the pseudo-first-order reaction rate constant (l/min). Meanwhile, the pseudo-second order kinetic model assumes that chemical adsorption can be the rate limiting stage involving valence forces through sharing or exchange of electrons between adsorbent and adsorbate (Zhang et al. 2014). The pseudo-second order equation depends on the adsorption equilibrium capacity which is expressed as below:

Linear:

$$\frac{t}{q_t} = \frac{1}{K_2 q_e^2} + \frac{t}{q_e} \quad (9)$$

Non-linear:

$$q_t = \frac{k^2 q_e{}^2 t}{1 + k^2 q_e t} \quad (10)$$

where K_2 is a constant that represents the pseudo-second order reaction rate equilibrium (g/mg min) (Fathi et al. 2020).

2.6. Desorption experiment

The reusability of the BBP adsorbent was assessed by desorption experiment. The manganese pre-sorbed BBP adsorbent samples (0.5g) were contacted with 100 ml of 0.5 M HCL in a conical flask and shaken at 150 rpm at room temperature. The sample was then collected at certain time interval and filter prior to be analysed for manganese concentration using ICP-OES.

3. Results and discussion

3.1. Characterization of BBP Adsorbent

3.1.1. Surface Morphology and EDX Analysis

The surface morphology, microstructures and physical properties of BBP adsorbent was determined using FESEM before and after Mn adsorption are depicted in Figure 2 and 3, respectively. The surface of BBP adsorbent is crimped with deeper dents, rough internals surface and dense in nature (Figure 2). The morphology of BBP may facilitate the adsorption of Mn owing to high irregular surface that provide maximum surface area for the adsorption of manganese ions (Fathi et al. 2020; Zhang et al. 2014; Abdeen et al. 2014; Bediako et al. 2019). Figure 2 and 3 shows the presence of prominent carbon (C), oxygen (O), and sodium (Na) elements from EDX analysis.

The BBP adsorbent's FESEM micrograph (Figure 3) reveals changes in shape indicating Mn^{2+} adsorption onto the BBP. The morphologies of FESEM in Figure 3 were observed to undergo changes after adsorption process where it has less crimped and rough surface compare to the pristine BBP adsorbent. The surfaces became loose porous might due to the vigorous shaking and interactions with the Mn solutions and water molecules creates micro-channels through Mn ions penetration to the internal binding sites (Bediako et al. 2019). Shiny particles were also observed over the surface of BBP after the adsorption takes place. Furthermore, the EDX spectra in Figure 3 detects an additional peak of Mn confirming the uptake of Mn ions onto the surface of BBP adsorbent.

3.1.2. FTIR Analysis

The functional groups detected in BBP adsorbent before and after manganese adsorption is shown in Figure 4 (a) and (b), respectively. Figure 4 (a) shows the broad transmission band at around 3288 cm^{-1} can be

attributed to the overlapping of hydroxyl group O–H (carboxylic acid), C-O stretching and N–H (amino groups) of macromolecular association (Mahmoud et al. 2014). The –OH or –NH stretch band was shifted to 3276 cm^{-1} which can be seen in Figure 4(b), implying that the adsorption involved –OH and C-O stretching of alcohol or –NH deformation (Chen et al. 2015). BBP contains C-H stretching vibration around 2915 cm^{-1} in Figure 4(a) that shift to 2919 cm^{-1} in Figure 4(b), which indicates the presence of an alkene functional group (Ashraf et al. 2017; Abdić et al. 2018). The changes of band at 1603 cm^{-1} (Figure 4(a)) to 1606 cm^{-1} (Figure 4(b)) is corresponding to the asymmetric stretching of the carboxylic C=O double bond, that is usually present in fibre materials containing pectin (Mahmoud et al. 2014). The peaks around 1245 cm^{-1} as seen in Figure 4(a) is due to C-O stretching vibrations in hemicellulose as well as C–O stretching vibration of acetyl group n lignin. The absent of 1245 cm^{-1} peak noticed in Figure 4(b) after the adsorption process pointed to the loss of hemicellulose and lignin (Mohamed et al. 2017). The changes of bands observed from 675 – 652 cm^{-1} in Figure 4(a) to a single band of 667 cm^{-1}, in Figure 4(b), may represents the aromatic C-H groups (Kim et al. 2020). The presence of functional groups (hydroxyl, carboxyl, amine, etc.) in BBP adsorbent had contribute to the adsorption processes of Mn.

3.1.3. XRD Analysis

XRD analysis of the BBP adsorbent before and after manganese adsorption is shown in Figure 5(a) and (b), respectively. Appearance of a broad low-intensity diffraction background and absence of sharp peaks, suggesting that the structure of BBP adsorbent is amorphous phase which related to the carbon structure (Bediako et al. 2019). Other than that, it is also due to organic materials and volatile substances. It was found that the presence of characteristic crystalline cellulose peaks manifested at $2\theta \approx 22^{o}$. The peak is attributed to the characteristics crystal structure of cellulose (Mahmoodi et al. 2018). After adsorption, no significant differences were observed in the crystalline peaks of the BBP adsorbent as in Figure 5(b), except that the intensity of the phases declined which indicate that manganese ions were replacing the ions and altering the structure of the BBP adsorbent. This demonstrates that adsorption of manganese did not change the structure space of BBP adsorbents and therefore the adsorption process occurred on the surface.

3.1.4. BET analysis

Adsorption is a complex phenomenon that depend on various factors including the pore structure, size, and surface chemistry of the adsorbent. The BET surface area for BBP adsorbent was 2.12 m^2/g with the total pore volume of 0.0139 cm^3/g and average pore diameter of 64.35 nm. Nitrogen adsorption-desorption isotherms

and pore size distribution curves (inset) of BBP adsorbent is shown in Figure 6. Based on the IUPAC classification, the isotherm for BBP adsorbent is classified as type 2 which is macropores (>50 nm). The pore size distribution makes it suitable for adsorbing manganese ions because it has an ionic radius about 0.80 nm (Goher et al. 2015). Therefore, manganese ions were able to enter the largest micropores (less than 2 nm according to IUPAC classification). The low surface area is a characteristic of most agro- or carbonaceous materials (Pathak and Kulkarni, 2017). However, the low surface area does not necessarily implying low adsorption potential of a material (Maia et al. 2021). The adsorption capacities of non-living biomasses are attributed mainly to the functional groups (amino, carbonyl, carboxyl) that present in the structure of the adsorbent (García-Mendieta and Solache-Ríos 2012).

3.2. Batch Adsorption Studies

3.2.1. Effect of pH

Figure 7 displays the optimal performance of various pH conditions with a 0.1-0.7g adsorbent dosage and initial manganese concentrations ranging from 10-50 mg/L in 60-180 min of contact time. The effect of pH ranges from 5-9 on the removal of Mn by the BBP adsorbent is shown in Figure 7(a). The surface charge on the BBP adsorbent can be used to explain the effect of pH. It was observed that the removal of Mn achieved at maximum of 90% at pH 7 as the initial pH was increased but gradually decreased over 7. The adsorption increased when the pH of the solution increased because more negative-charged; metal-binding sites were exposed, attracting positive-charged metal ions and inducing adsorption onto the adsorbent surface (Mumtaz et al. 2014). The positive charge density of H^+ ion decreases with increasing pH, which reduces electrostatic repulsion on the surface of BBP adsorbent and attracts more manganese ions, thus facilitating greater metal adsorption (Adekola et al. 2016). The lowest percentage removal of Mn^{2+} was found at pH 4 and pH 5.5. This can be explained by the fact that the high H^+ ion concentration at low pH occupies most of the adsorbent's active sites, thus lowering manganese ion removal efficiency (Abdić et al. 2018). Saturation of the bonded active sites took place and became inaccessible to other cations (Fathi et al. 2020). According to Akl et al. (2013), pH solution strongly affects the surface charge on the solid particles. In addition, it also changes the properties and availability of metal ions in solution, as well as the chemical state of the functional groups during the adsorption process (Abdić et al. 2018). This could be attributed to the partial hydrolysis of Mn^{2+} ions with increasing pH that results in the formation of complexes OH^- such as $Mn(OH)^+$, $Mn(OH)_2$, $Mn_2(OH)_3^+$ and Mn_2OH^{3+} species in solution. Therefore, the

adsorption and precipitation of manganese-hydroxyl species into the adsorbent structure may be involved (Esfandiar et al. 2014). The dependency of Mn adsorption at higher pH is associated with the surface functional groups of the BBP adsorbent and the metal chemistry in the solution where the functional groups can be seen in the previous section in Figure 4. According to Feizi and Jalali (2015), dissociation of specific functional groups such as carboxyl and hydroxyl is important in metal sorption. As the pH increased, the functional groups would be exposed, increasing the density of negative charge on the surface of BBP adsorbent that contributes to the attraction between manganese ions and functional groups (Fathi et al. 2020). The adsorption capacity of BBP adsorbent is based on the pH value, together with surface charge and ionisation. Therefore, pH 7 is the optimum pH value for maximum Mn removal in the present study

3.2.2 Effect of Initial Manganese Concentration

The effect of initial Mn ion concentration of 10 – 50 mg/L are depicted in Figure 7(b) where BBP adsorbent solution was employed with the optimal pH 8 as shown in the previous section. It was perceived that the percentage of Mn removal decreases with the increase of initial Mn ions concentration. The initial of Mn concentration of 20 mg/L showed the total Mn removal of 100%. A trend was observed in Figures 7(b)where Mn removal was decreased from 100% to 32%, with increased initial Mn concentration from 10–50 mg/L, respectively. This indicates that the surface saturation is dependent on the initial manganese concentration. The adsorbent surface area saturates at higher manganese concentration as the diffusion of the ions from the bulk solution to the adsorbent surface area decreases (Ali et al. 2017). Idrees et al. (2018) suggested that initial manganese ion concentration gives an impelling cause to overcome metal transfer resistances in the adsorbent and solution. This leads to a collision of higher probability between the active sites of BBP adsorbent and manganese ions. The adsorption sites become occupied at some point and reach a constant value where further adsorption from an aqueous solution is impossible. Adeogun et al. (2013) also showed that the removal of Mn ions using raw and oxalic acid modified rice husk adsorbent decreased with the increase in initial Mn concentration. Initially, adsorption occurs rapidly on the adsorbent's external surface, followed by a slower internal diffusion process, which may be the rate-determining step. This is comparable with this study, where the rate of adsorption is fast in the first 10 minutes, until almost equilibrium due to quick occupancy of Mn ions onto the surface of BBP adsorbent

3.2.3 Effect of Adsorbent Dosage

The effect of BBP dosage on the removal of manganese with the optimal initial Mn concentration of 20 mg/L, at pH 7 is shown in Figure 7(c). The adsorbent dosage was employed from 0.1 g/L to 0.7 g/L and the experiments were shaken for 150 minutes. The obtained findings indicate that as the adsorbent dose is raised, the efficacy of Mn removal improves. The greatest Mn removal was 96% at the optimum adsorbent dosage of BBP (0.5 g/L). High adsorbent dosage provides more active exchangeable adsorption sites. However, excessive adsorbent dosage could also decrease the adsorption rate due to interference caused by the interaction of active sites of the adsorbent (Iftekhar et al. 2018). Abdić et al.(2018) showed that the increase in the amount of tangerine peels adsorbent had increased the Mn removal efficiencies. This situation is because higher adsorbent dosage provides greater surface area and more metal-binding sites. Therefore, the rate of Mn adsorption was increased even when the initial metal concentration remained constant (Esfandiar et al. 2014). Furthermore, Mahmoud et al. (2014) also reported that increasing the banana peel activated carbon (BPAC) adsorbent dosage led to higher manganese adsorption. This can be attributed to the presence of more binding surfaces for manganese ions and the increased surface area (Ahmed et al, 2015). The effective surface area for adsorption was increased by increasing the adsorbent dosage (Adekola et al. 2014).

3.2.4 Effect of Contact Time

The time plays a vital role in the adsorption by BBP which was investigated within a time period of 30-180 minutes in 250 mL of solution; 0.5 g/L (BBP), initial Mn concentration of 20 mg/L and a pH of 7. Determination of the optimal contact time is done after the optimum pH and initial concentration are determined (Kurniawati et al. 2021). Figure 7(d) shows that the optimum time of adsorption of Mn by BBP achieved 100% of total removal when the contact time increased up to 150 minutes after equilibrium was achieved. Similar findings were reported by Hegazy et al. (2021) that removed 93% of Mn within 120 minutes contact time until it reached equilibrium by using *Moringa oleifera* seeds adsorbent.

According to the findings of this experiment, adsorption occurs in two stages, the first is rapid adsorption and the second of which is the delayed release of adsorbent compounds. This is because the amount of adsorbed Mn has exceeded the maximum number of Mn that adsorbents have reached saturation. If a lot of adsorbents have

saturated the active site on the surface of the adsorbent, further adsorption time will no longer increase the adsorption and even tends to reduce it (Kurniawati et al. 2021).

3.3 Comparison with previous studies on Mn removal under optimum conditions

The result obtained under optimal Mn removal conditions for BBP in the previous experiments was performed to validate the optimal conditions. The validation experiment was conducted at 0.5g of BBP adsorbent dose, initial Mn concentration of 20 mg/L at pH 7, and agitated for 150 minutes at 125 rpm. The results were close to the previous experiment with 98% Mn removal and clearly showed that the factors affecting the adsorption process for Mn removal was successfully determined. Table 1 shows BBP adsorbent has remarkable adsorption capacity as compared to other studies in the literature.

3.4 Adsorption Isotherm Studies

The adsorption relationships analysis using Langmuir and Freundlich isotherm for the adsorption of Mn are depicted in Figure 8. The experiment for both isotherms for Mn removal was analysed under optimised conditions as mentioned in the previous section. These two models have the simplest experimental activities of a wide range of operating conditions. According to the Langmuir isotherm, the uptake occurs on a homogeneous surface through monolayer sorption with no interaction between the adsorbed molecules (Mahmoud et al. 2014). Langmuir and Freundlich linear model were best fitted according to the predicted adsorption equilibrium as the correlation coefficients of R^2 analysis; 0.984 (linear Langmuir) and 0.995 (linear Freundlich) compare to non-linear Langmuir (0.388) and non-linear Freundlich (0.516), respectively.

Table 2 displayed the Langmuir and Freundlich constant isotherm on the established coefficient of R^2 from the basis of the modelling curve. From the plot in Figure 8 (a) and (c), the correlation coefficients of R^2 and the value calculated for q_{max} is close to the experimental q_{max}, thus showing that the data fit to the linear Langmuir model. The R_L value that is between 0 and 1 ($0< R_L <1$), implied that the process is favourable (Adeogun et al. 2013). On the other hand, the determination correlation coefficients of R^2 in linear Freundlich model was also in a good fit for the experimental data whereas the value of value of $1/n < 1$ indicates that the process is favourable adsorption and the surface of adsorbent is highly heterogeneous (Adeogun et al. 2013).

The isotherm results obtained in the present study can be concluded that the experimental data for adsorption of Mn ions onto BBP adsorbent fitted to both linear isotherm model as the values for the correlation

coefficients (R^2) were both high (R^2>0.98). The Mn adsorption behaviour on BBP adsorbent may occur in multilayers on the surface of the adsorbent. However, based on the satisfactory correlation coefficients, the data is also consistent with linear on both isotherm models in which the monolayer adsorption takes place on the BBP adsorbent.

3.5 Adsorption Kinetics

The graph of linear and non-linear of Pseudo-first order and second order kinetic is plotted in Figure 9, respectively. The regression coefficient must be high (R^2) and the calculated q_e values should be closed to the experimental q_e (Marque et al. 2013). These criteria must be satisfied in order to be fitted in these kinetic models. The kinetics adsorption of Mn onto the BBP adsorbent was well represented by the pseudo-second order whereas the linear and non-linear of Pseudo first order was unsuitable due to the low R^2 values. The graph of Pseudo-first order in Figure 9 (a and c) shows poor correlation of parameters with R^2 = 0.840 (linear) and R^2= 0.875 (non-linear) while the graph for pseudo-second order was best described in Figure 9 (c) with high linear regression of R^2 = 0.99

Table 2 represent the linear pseudo-second order is predominant kinetic model for the Mn adsorption by BBP adsorbent due to higher value of R^2 than those in pseudo-first order. Furthermore, the pseudo-second order calculated q_e values are in good agreement with the experimental q_e values compared in the pseudo-first order model. Thus, this confirms that chemisorption of manganese onto the BBP adsorbent is the main mechanism in the adsorption process (Adekola et al. 2020; Zhang et al. 2014). In chemisorption, a chemical bond (usually covalent) is formed as metal ions adhere to adsorbent surface that also increase coordination number with the surface (Senthil et al. 2010). Based on the FTIR results (refer Section 3.1.3), hydroxyl and carboxyl were abundance and involved in chemical bonding. The possible ion exchange mechanisms is when Mn ion attached itself to two adjacent hydroxyl groups and two-oxyl groups which could donate two pairs of electrons to the metal ions, hence forming four coordination number compounds and releasing two hydrogen ions into solution (Omri and Benzina, 2019).

3.6 Desorption studies

Figure 10 shows the desorption of manganese by BBP adsorbent. The experiment was run at optimum condition obtain in adsorption study which is at 0.1M HCL acid, 0.5g BBP adsorbent, and 150 mins. Low concentration of HCL acid was used for effective desorption process as the reaction is more stable. In the first

cycle, high desorption of manganese of 92% was attained in 30 minutes. The recovery of BBP adsorbent by using HCL acid demonstrate high percentage of manganese desorbed in 5 minutes and reach maximum in 30 minutes. However, the desorption efficiency was decreased to 51% in the second cycle and further decreased to 32% in the third cycle. The loss rate after the third cycle desorption was 60%. This might be due to the reduction of functional groups in BBP adsorbent surface and incomplete desorption during the regeneration process. Long-term elution can destroy the binding site or leave manganese ions in the adsorbent (Li et al. 2021).

Figure 11 shows the recovery of BBP adsorbent for manganese removal. The recovery rate in the first cycle was 94.18% and decreased to 61.38% in the second cycle followed by 40.39% in the third cycle. This showed that the adsorption recovery was effective in the first cycle but was gradually decreased in the second and third cycle. These finding shows that BBP adsorbent has potential reusability and efficient for reused after the first cycle of desorption process. Increasing of desorption cycles lead to gradual destruction of the active binding sites on the adsorbent after each cycle. Therefore, the performance of the regenerated adsorbent is not comparable with the freshly prepared adsorbent. The decrease of desorption efficiency can also be caused by the saturation and occupation of adsorption sites with strongly adsorbed adsorbate (Vakili et al. 2019). Moreover, some chemical reagents could change the chemical structure of adsorbents by interacting with some constituents of the adsorbent (Omorogie et al. 2016). This will decrease adsorption capacity of the adsorbent as HCL acid could weaken some active sites in the adsorbent by leaching some ions into the desorbing solution with each desorbing cycle.

4. Conclusion

The chemical modified BBP adsorbent resulted in large surface area and crumpled shape of the adsorbent that cater for maximum adsorption rate. FTIR analysis reveals the presence of hydroxyl and carboxyl group that plays important role in adsorption process. XRD analysis suggests that the structure of BBP is amorphous while BET analysis indicate that the size distribution of BBP adsorbent is macropores. Isotherm studies show the experimental data was well presented by the linear Langmuir and Freundlich model. Additionally, the linear pseudo-second order provides a well linear regression with R^2 of 0.99. Hence, the mechanism for the adsorption of manganese by the BBP adsorbent is by chemisorption where the Mn ions adhere to the surface of BBP adsorbent by chemical bond. The efficiency of reusing BBP adsorbent for further adsorption process is after the first desorption cycle with the highest recovery rate of 94.18%. According to the findings, BBP adsorbent is a potential natural adsorbent that is effective for treating water containing Mn at the optimum condition. Furthermore, the

455 ability of the BBP adsorbent to be reused demonstrated that the adsorbent is economical and can reduce negative
456 impact to the environment.

457 **Acknowledgement**

458 The authors thank the parties involved in this project, especially Universiti Tun Hussein Onn Malaysia,
459 for providing the research facilities and equipment. The authors wish to thank the Ministry of Higher Education
460 Malaysia for the Fundamental Research Grant Scheme grant (K219) (FRGS/1/2019/TK10/UTHM/03/3).

461

References

Abdeen Z, Mohammad SG, Mahmoud MS (2015) Adsorption of Mn (II) ion on polyvinyl alcohol/chitosan dry blending from aqueous solution. Environmental Nanotechnology, Monitoring & Management 3:1-9. https://doi.org/10.1016/j.enmm.2014.10.001

Abdić Š, Memić M, Šabanović E, Sulejmanović J, Begić S (2018) Adsorptive removal of eight heavy metals from aqueous solution by unmodified and modified agricultural waste: tangerine peel. International Journal of Environmental Science and Technology 5(12):2511-8. https://doi.org/10.1007/s13762-018-1645-7

Adekola FA, Hodonou DS, Adegoke HI (2016) Thermodynamic and kinetic studies of biosorption of iron and manganese from aqueous medium using rice husk ash. Applied Water Science 4:319-30. https://doi.org/10.1007/s13201-014-0227-1

Adeogun AI, Idowu MA, Ofudje AE, Kareem SO, Ahmed SA (2013) Comparative biosorption of Mn (II) and Pb (II) ions on raw and oxalic acid modified maize husk: kinetic, thermodynamic and isothermal studies. Applied Water Science 167-79. https://doi.org/10.1007/s13201-012-0070-1

Ahmadi S, Ganjidoust H (2021) Using banana peel waste to synthesize BPAC/ZnO nanocomposite for photocatalytic degradation of Acid Blue 25: Influential parameters, mineralization, biodegradability studies. Journal of Environmental Chemical Engineering 9(5):106010. https://doi.org/10.1016/j.jece.2021.106010

Ahmed F, Siwar C, Begum RA (2014) Water resources in Malaysia: Issues and challenges. J. Food Agric. Environ 12(2):1100-4.

Ahmed SA, El-Roudi AM, Salem AA (2015) Removal of Mn (II) from ground water by solid wastes of sugar industry. Journal of Environmental Science and Technology 8(6):338. https://doi.org/10.3923/jest.2015.338.351

Akl MA, Yousef AM, AbdElnasser S (2013) Removal of iron and manganese in water samples using activated carbon derived from local agro-residues. J. Chem. Eng. Process Technol 4(04). https://doi.org/10.4172/2157-7048.1000154

Ali A. Removal of Mn (II) from water using chemically modified banana peels as efficient adsorbent (2017) Environmental Nanotechnology, Monitoring & Management 7:57-63. https://doi.org/10.1016/j.enmm.2016.12.004

Al-Jubouri SM, Holmes SM (2017) Hierarchically porous zeolite X composites for manganese ion-exchange and solidification: Equilibrium isotherms, kinetic and thermodynamic studies. Chemical Engineering Journal 308:476-91. https://doi.org/10.1016/j.cej.2016.09.081

Alvarez-Bastida C, Martínez-Miranda V, Solache-Ríos M, Linares-Hernández I, Teutli-Sequeira A, Vázquez-Mejía G (2018) Drinking water characterization and removal of manganese. Removal of manganese from water. Journal of Environmental Chemical Engineering 6(2):2119-25.

https://doi.org/10.1016/j.jece.2018.03.019

Ashraf A, Bibi I, Niazi NK, Ok YS, Murtaza G, Shahid M, Kunhikrishnan A, Li D, Mahmood T (2017) Chromium (VI) sorption efficiency of acid-activated banana peel over organo-montmorillonite in aqueous solutions. International journal of phytoremediation. 19(7):605-13. https://doi.org/10.1080/15226514.2016.1256372

Bangaraiah P (2018) Biosorption of manganese using tamarind fruit shell powder as a biosorbent. Research Journal of Pharmacy and Technology 11(10):4313-6. https://doi.org/10.5958/0974-360X.2018.00789.8.

Baysal A, Ozbek N, Akman S (2013) Determination of trace metals in waste water and their removal processes. Waste Water-Treatment Technologies and Recent Analytical Developments 145-71. http://dx.doi.org/10.5772/52025

Bediako JK, Sarkar AK, Lin S, Zhao Y, Song MH, Choi JW, Cho CW, Yun YS (2019) Characterization of the residual biochemical components of sequentially extracted banana peel biomasses and their environmental remediation applications. Waste management 89:141-53. https://doi.org/10.1016/j.wasman.2019.04.009

Bouchard MF, Surette C, Cormier P, Foucher D (2018) Low level exposure to manganese from drinking water and cognition in school-age children. Neurotoxicology 64:110-7. https://doi.org/10.1016/j.neuro.2017.07.024

Carolin CF, Kumar PS, Saravanan A, Joshiba GJ, Naushad M (2017) Efficient techniques for the removal of toxic heavy metals from aquatic environment: A review. Journal of environmental chemical engineering 5(3):2782-99. https://doi.org/10.1016/j.jece.2017.05.029

Chen L, Fang Y, Jin Y, Chen Q, Zhao Y, Xiao Y, Zhao H (2015) Biosorption of Cd2+ by untreated dried powder of duckweed Lemna aequinoctialis. Desalination and Water Treatment 53(1):183-94. https://doi.org/10.1080/19443994.2013.839399

Du X, Zhang K, Xie B, Zhao J, Cheng X, Kai L, Nie J, Wang Z, Li G, Liang H (2019) Peroxymonosulfate-assisted electro-oxidation/coagulation coupled with ceramic membrane for manganese and phosphorus removal in surface water. Chemical Engineering Journal365:334-43. https://doi.org/10.1016/j.cej.2019.02.028

Esfandiar N, Nasernejad B, Ebadi T (2014) Removal of Mn (II) from groundwater by sugarcane bagasse and activated carbon (a comparative study): application of response surface methodology (RSM). Journal of industrial and engineering chemistry. 20(5):3726-36. https://doi.org/10.1016/j.jiec.2013.12.072

Seyedpour, S. F., Rahimpour, A., Mohsenian, H., & Taherzadeh, M. J. (2018). Low fouling ultrathin nanocomposite membranes for efficient removal of manganese. Journal of Membrane Science, 549, 205-216. https://doi.org/10.1016/j.memsci.2017.12.012

Fathi A, Gahlan AA, Farghaly OA (2020) Decontamination of Copper and Manganese from Aqueous Media by Untreated and Chemically Treated Sugarcane Bagasse: A Comparative Study. Chemistry of Advanced

Materials 5(2).

Feizi M, Jalali M (2015) Removal of heavy metals from aqueous solutions using sunflower, potato, canola and walnut shell residues. Journal of the Taiwan Institute of Chemical Engineers 54:125-36. https://doi.org/10.1016/j.jtice.2015.03.027

García-Mendieta A, Olguín MT, Solache-Ríos M (2012) Biosorption properties of green tomato husk (Physalis philadelphica Lam) for iron, manganese and iron–manganese from aqueous systems. Desalination. 2012 Jan 4;284:167-74. https://doi.org/10.1016/j.desal.2011.08.052

Gerke TL, Little BJ, Maynard JB (2016) Manganese deposition in drinking water distribution systems. Science of the Total Environment 541:184-93. https://doi.org/10.1016/j.scitotenv.2015.09.054

Goher ME, Hassan AM, Abdel-Moniem IA, Fahmy AH, Abdo MH, El-sayed SM (2015) Removal of aluminum, iron and manganese ions from industrial wastes using granular activated carbon and Amberlite IR-120H. The Egyptian Journal of Aquatic Research. 2015 Jan 1;41(2):155-64. https://doi.org/10.1016/j.ejar.2015.04.002

Gopakumar A, Narayan R, Nagath SA, Nishanthan P (2018) Waste Water Treatment Using Economically Viable Natural Adsorbent Materials. Materials Today: Proceedings5(9):17699-703. https://doi.org/10.1016/j.matpr.2018.06.091 \

Ihsanullah, Abbas, A., Al-Amer, A. M., Laoui, T., Al-Marri, M. J., Nasser, M. S., Khraisheh, M., & Atieh, M. A. (2016). Heavy metal removal from aqueous solution by advanced carbon nanotubes: critical review of adsorption applications. Separation and Purification Technology, 157, 141-161. https://doi.org/10.1016/j.seppur.2015.11.039

Hegazy I, Ali ME, Zaghlool EH, Elsheikh R (2021) Heavy metals adsorption from contaminated water using Moringa seeds/olive pomace byproducts. Applied Water Science. 11(6):1-4. https://doi.org/10.1007/s13201-021-01421-5

Herawati D, Santoso SD, Amalina I (2018) Kondisi Optimum Adsorpsi-fluidisasi Zat Warna Limbah Tekstil Menggunakan Adsorben Jantung Pisang. Jurnal SainHealth 2(1):1-7. http://dx.doi.org/10.51804/jsh.v2i1.169.1-7

Idrees M, Batool S, Ullah H, Hussain Q, Al-Wabel MI, Ahmad M, Hussain A, Riaz M, Ok YS, Kong J (2018) Adsorption and thermodynamic mechanisms of manganese removal from aqueous media by biowaste-derived biochars. Journal of Molecular Liquids 266:373-80. https://doi.org/10.1016/j.molliq.2018.06.049

Iftekhar S, Ramasamy DL, Srivastava V, Asif MB, Sillanpää M (2018) Understanding the factors affecting the adsorption of Lanthanum using different adsorbents: a critical review. Chemosphere. 204:413-30. https://doi.org/10.1016/j.chemosphere.2018.04.053

Jawed A, Pandey LM (2019) Application of bimetallic Al-doped ZnO nano-assembly for heavy metal removal and decontamination of wastewater. Water Science and Technology 80(11):2067-78.

https://doi.org/10.2166/wst.2019.393

Jeirani Z, Sadeghi A, Soltan J, Roshani B, Rindall B (2015) Effectiveness of advanced oxidation processes for the removal of manganese and organic compounds in membrane concentrate. Separation and Purification Technology 149:110-5. https://doi.org/10.1016/j.seppur.2015.05.009

Kim H, Ko RA, Lee S, Chon K (2020) Removal efficiencies of manganese and iron using pristine and phosphoric acid pre-treated biochars made from banana peels. Water. 12(4):1173. https://doi.org/10.3390/w12041173

Kurniawati D, Sari TK, Adella F, Sy S (2021) Effect of Contact Time Adsorption of Rhodamine B, Methyl Orange and Methylene Blue Colours on Langsat Shell with Batch Methods. InJournal of Physics: Conference Series 2021 Feb 1 (Vol. 1788, No. 1, p. 012008). IOP Publishing. https://doi.org/10.1088/1742-6596/1788/1/012008

Li X, Yu X, Liu L, Yang J, Liu S, Zhang T (2021) Preparation, characterization serpentine-loaded hydroxyapatite and its simultaneous removal performance for fluoride, iron and manganese. RSC Advances. 2021;11(27):16201-15. https://doi.org/10.1039/D1RA02028E

Mahmoodi NM, Taghizadeh M, Taghizadeh A (2018) Mesoporous activated carbons of low-cost agricultural bio-wastes with high adsorption capacity: preparation and artificial neural network modeling of dye removal from single and multicomponent (binary and ternary) systems. Journal of Molecular Liquids 269:217-28. https://doi.org/10.1016/j.molliq.2018.07.108

Mahmoud MS, Ahmed SM, Mohammad SG, Abou Elmagd AM (2014) Evaluation of Egyptian banana peel (Musa sp.) as a green sorbent for groundwater treatment. International Journal of Engineering and Technology (11):648-59.

Maia LS, Duizit LD, Pinhatio FR, Mulinari DR (2021) Valuation of banana peel waste for producing activated carbon via NaOH and pyrolysis for methylene blue removal. Carbon Letters 1-4. https://doi.org/10.1007/s42823-021-00226-5

Marques TL, Alves VN, Coelho LM, Coelho NM (2013) Assessment of the use of Moringa oleifera seeds for removal of manganese ions from aqueous systems. BioResources 8(2):2738-51.

Marsidi N, Hasan HA, Abdullah SR (2018) A review of biological aerated filters for iron and manganese ions removal in water treatment. Journal of Water Process Engineering 23:1-2. https://doi.org/10.1016/j.jwpe.2018.01.010

Meseldžija S, Petrović J, Onjia A, Volkov-Husović T, Nešić A, Vukelić N (2020) Removal of Fe2+, Zn2+ and Mn2+ ions from the mining wastewater by lemon peel waste. Journal of the Serbian Chemical Society. 2020;85(10):1371-82. https://doi.org/10.2298/JSC200413030M

Milatovic D and Gupta RC, (2018) “Manganese,” in Veterinary Toxicology: Basic and Clinical Principles: Third Edition, Third Edit., Elsevier Inc., 445–454.

Mohamed RM, Hashim N, Abdullah S, Abdullah N, Mohamed A, Daud MA, Muzakkar KF (2020) Adsorption

598 of Heavy Metals on Banana Peel Bioadsorbent. In Journal of Physics: Conference Series 2020 Jun 1 (Vol.
599 1532, No. 1, p. 012014). IOP Publishing. https://doi.org/10.1088/1742-6596-1532-1-012014

600 Mthombeni NH, Mbakop1and S, Onyango MS. Adsorptive removal of manganese from industrial and mining
601 wastewater (2016) InProceedings of Sustainable Research and Innovation Conference pp. 36-45.

602 Mumtaz MW, Mukhtar H, Anwar F, Saari N (2014) RSM Based Optimization of Chemical and Enzymatic
603 Transesterification of Palm Oil : Biodiesel Production andAssessment of Exhaust Emission Levels, Sci.
604 World J., 1–11.

605 Omorogie MO, Babalola JO, Unuabonah EI (2016) Regeneration strategies for spent solid matrices used in
606 adsorption of organic pollutants from surface water: a critical review. Desalination and water treatment.
607 57(2):518-44. https://doi.org/10.1080/19443994.2014.967726

608 Omri A, Benzina M (2012) Removal of manganese (II) ions from aqueous solutions by adsorption on activated
609 carbon derived a new precursor: Ziziphus spina-christi seeds. Alexandria Engineering Journal51(4):343-
610 50. https://doi.org/10.1016/j.aej.2012.06.003

611 Pathak PD, Mandavgane SA, Kulkarni BD (2017) Fruit peel waste: characterization and its potential uses. Current
612 Science 444-54.

613 Rumsby P, Rockett L, Clegg H, Jonsson J, Benson V, Harman M, Doyle T, Rushton L, Wilkinson D, Warwick P
614 (2014) Speciation of manganese in drinking water. Toxicology Letters (229):S120.
615 https://doi.org/10.1016/j.toxlet.2014.06.431

616 Kumar, P. S., Vincent, C., Kirthika, K., & Kumar, K. S. (2010). Kinetics and equilibrium studies of Pb2+ in
617 removal from aqueous solutions by use of nano-silversol-coated activated carbon. Brazilian Journal of
618 Chemical Engineering, 27(2), 339-346. https://doi.org/10.1590/S0104-66322010000200012

619 Singh NB, Nagpal G, Agrawal S (2018) Water purification by using adsorbents: a review. Environmental
620 technology & innovation 11:187-240. https://doi.org/10.1016/j.eti.2018.05.006

621 Surovka D, Pertile E (2017) Sorption of Iron, Manganese, and Copper from Aqueous Solution Using Orange Peel:
622 Optimization, Isothermic, Kinetic, and Thermodynamic Studies. Polish Journal of Environmental Studies
623 26(2). https://doi.org/10.15244/pjoes/60499

624 Tobiason, J.E., Bazilio, A., Goodwill, J., Mai, X., and Nguyen, C. (2016) Manganese Removal from Drinking
625 Water Sources. *Current Pollution Reports*, **2**, 168–177. Current Pollution Reports.
626 https://doi.org/10.1007/s40726-016-0036-2

627 Vakili M, Deng S, Cagnetta G, Wang W, Meng P, Liu D, Yu G (2019) Regeneration of chitosan-based adsorbents
628 used in heavy metal adsorption: A review. Separation and Purification Technology 224:373-87.
629 https://doi.org/10.1016/j.seppur.2019.05.040

630 Zhang Y, Zhao J, Jiang Z, Shan D, Lu Y (2014) Biosorption of Fe (II) and Mn (II) ions from aqueous solution by
631 rice husk ash. Biomed research international. 2014. https://doi.org/10.1155/2014/973095

632 Zou Y, Wang X, Khan A, Wang P, Liu Y, Alsaedi A, Hayat T, Wang X (2016) Environmental remediation and
633 application of nanoscale zero-valent iron and its composites for the removal of heavy metal ions: a review.
634 Environmental science & technology 50(14):7290-304. https://doi.org/10.1021/acs.est.6b01897

635

List of Table

Table 1 Comparison of the present study findings with previous studies.

Adsorbent	Manganese removal (%)	pH	Contact time (min)	Adsorbent dosage (g)	Mn conc. (mg/L)	References
Moringa seed	93	5	120	5	50	(Hegazy et al. 2021)
Olive pomace	91	5	120	5	50	(Hegazy et al. 2021)
Biochar-banana peel	46	7	180	3	10	(Kim et al. 2020)
Lemon peel	78.2	4	15	1	25	(Meseldzija et al. 2020)
Beet pulp	86.4	6	90	1	2	(Ahmed et al. 2015)
Tamarind fruit shell	74	3	60	1.2	100	(Bangaraiah, 2018)
Sugarcane Bagasse	62.5	6	150	0.15	2	(Ahmed et al. 2015)
BBP	98	7	150	0.5	20	This study

Table 2 Langmuir and Freundlich isotherm equilibrium parameters for manganese adsorption onto BBP adsorbent

Model	Parameters	Non-linear	Linear
Langmuir	q_{max}	15	15.089
	R_L	2.14	0.02
	R^2	0.388	0.984
Freundlich	1/n	0.2365	0.25
	kf	8	2.294
	R^2	0.516	0.995
Pseudo-first order	qe	14.15	62.783
	K_1	1.81	2.04
	R^2	0.875	0.840
Pseudo-second order	qe	14.33	14.547
	K_1	1.671	0.881
	R^2	0.899	0.991

List of Figure

Figure 1 Schematic of BBP adsorbent preparation via chemical treatment

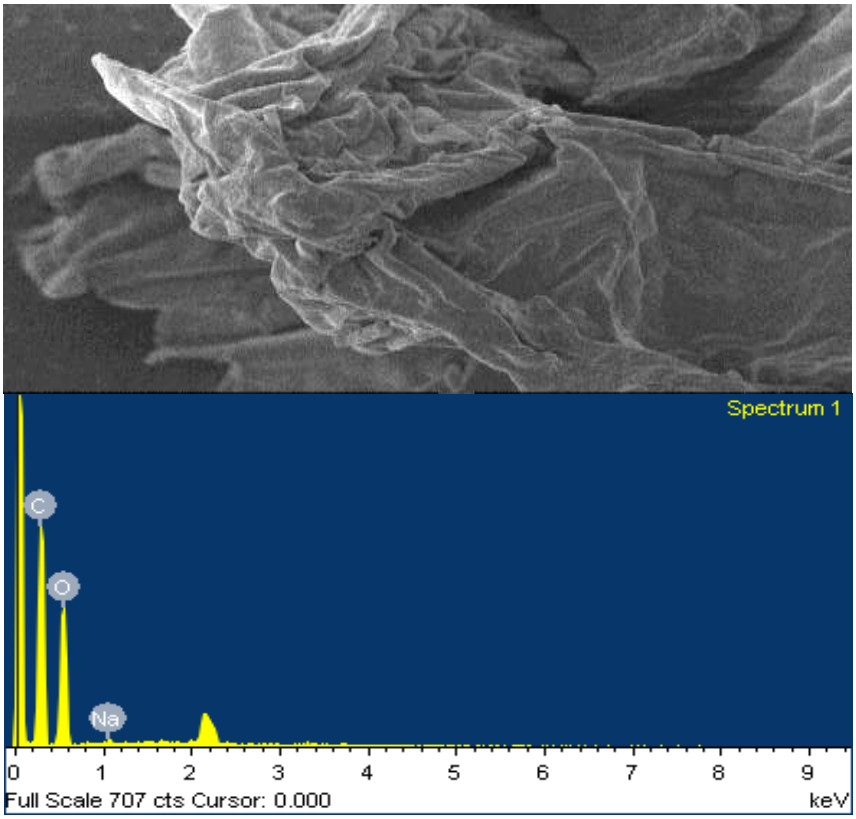

664

665 **Figure 2** Scanning Electron Microscopic of pristine BBP adsorbent before adsorption of Mn with EDX analysis

666

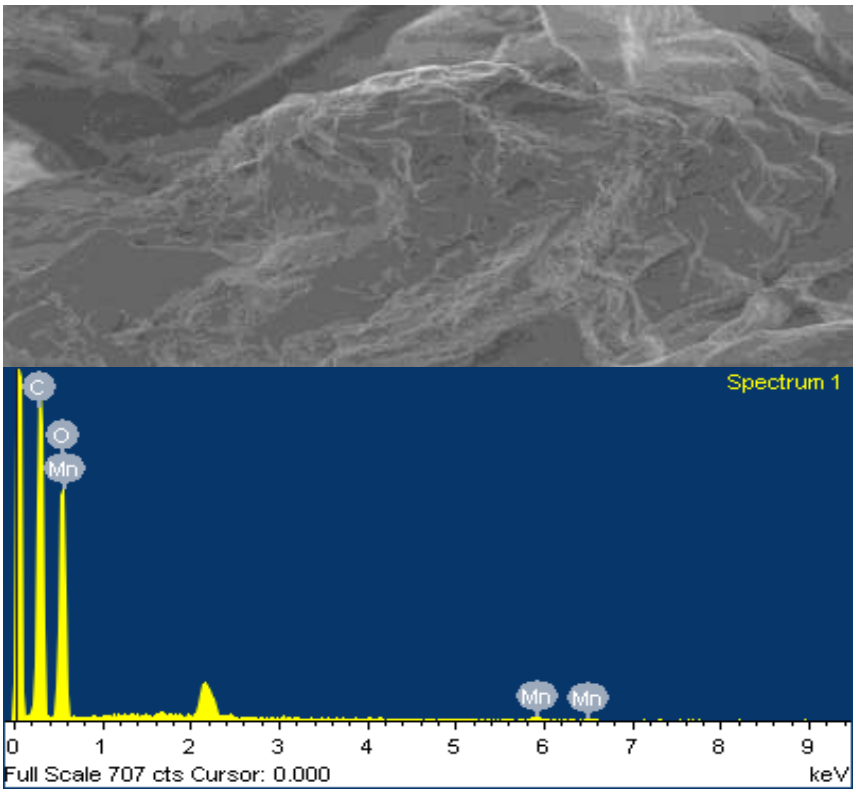

667

668 **Figure 3** Scanning Electron Microscopic of BBP adsorbent after adsorption of Mn with EDX analysis

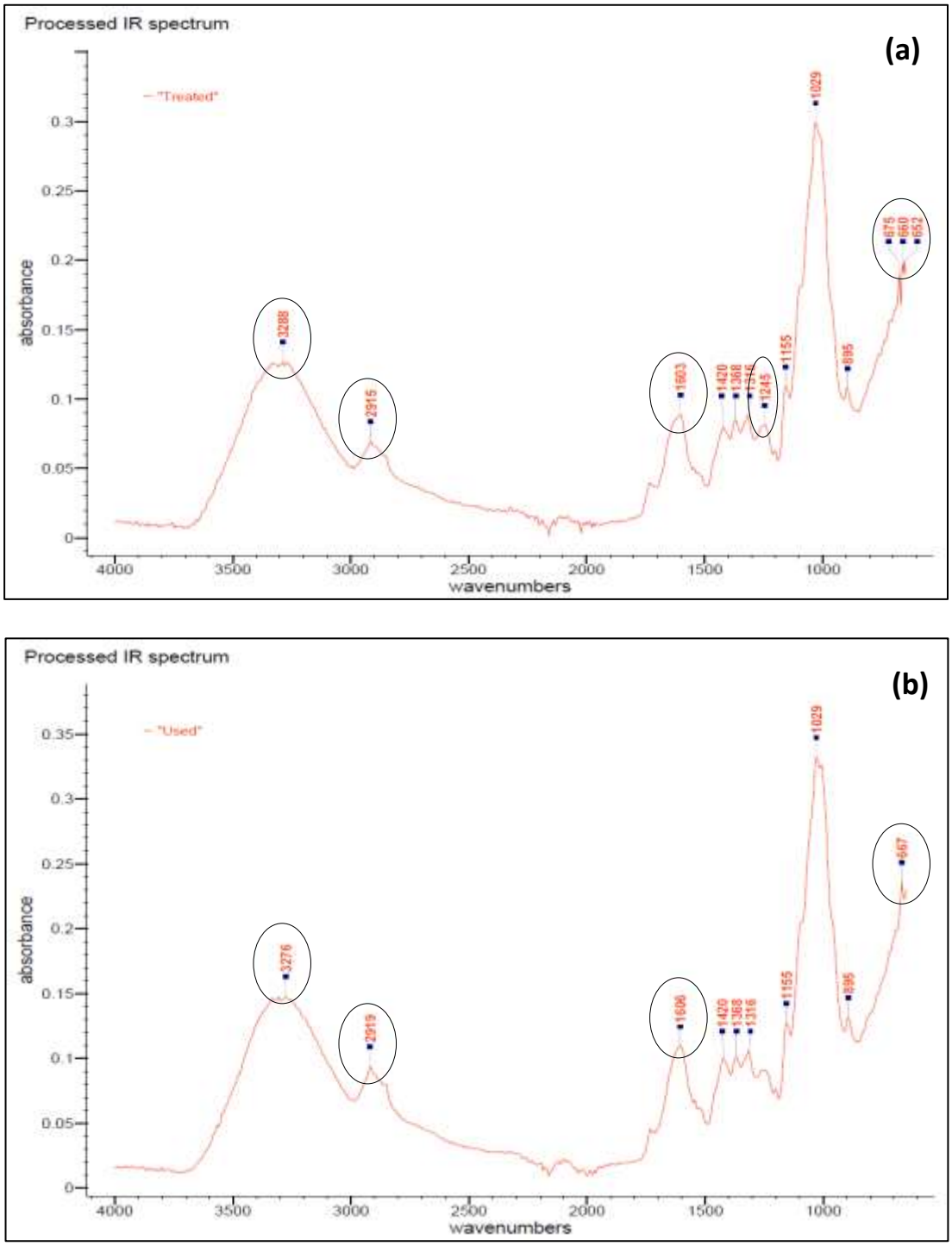

669

670 **Figure 4** FTIR analysis of BBP adsorbent (a) before and (b) after manganese adsorption

671

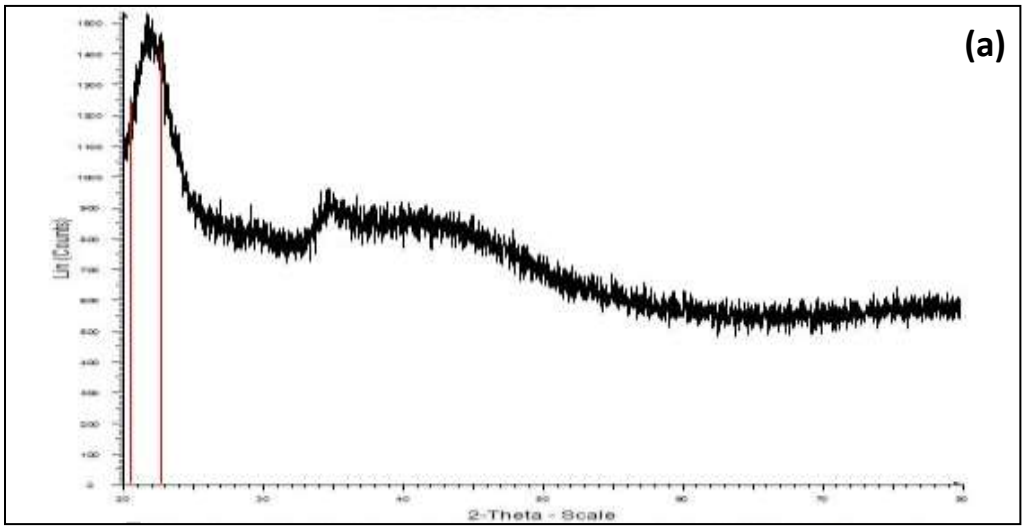

672

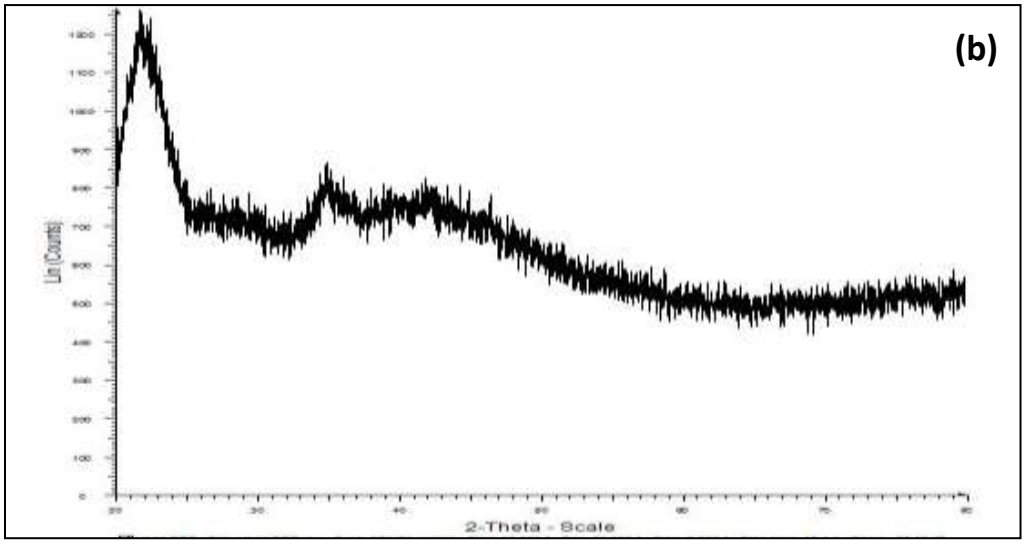

673

674 **Figure 5** XRD pattern of BBP adsorbent (a) before and (b) after manganese adsorption

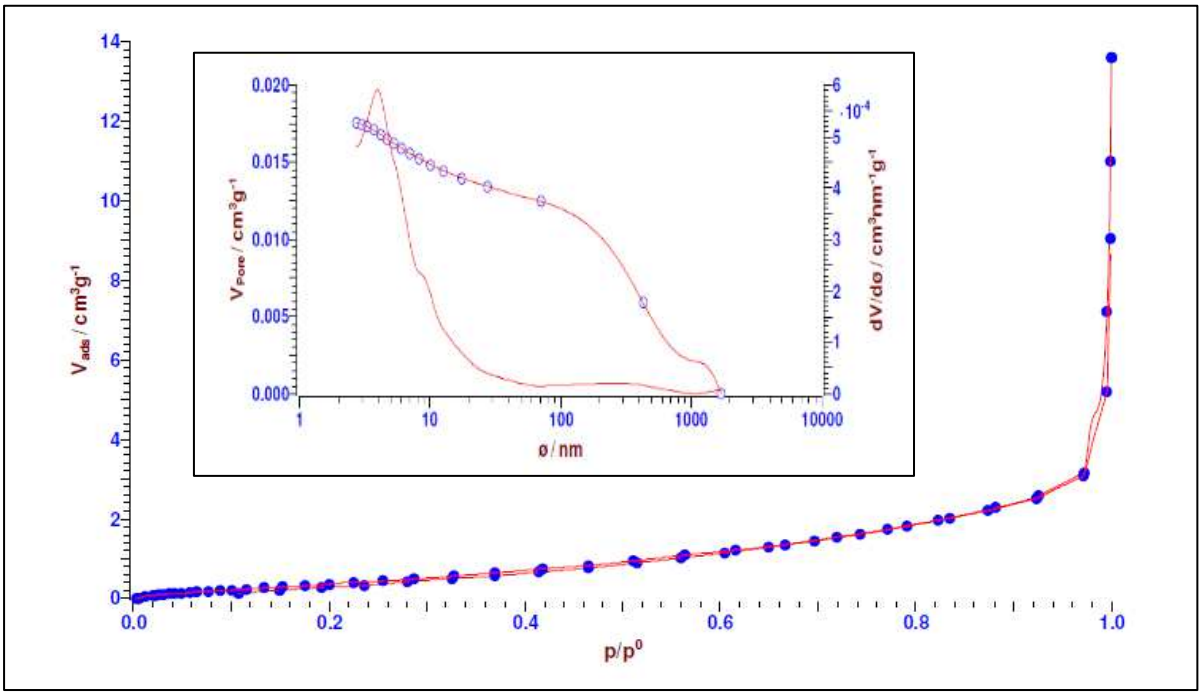

675

676 **Figure 6** Nitrogen adsorption-desorption isotherms and pore size distribution curves (inset) of BBP adsorbent

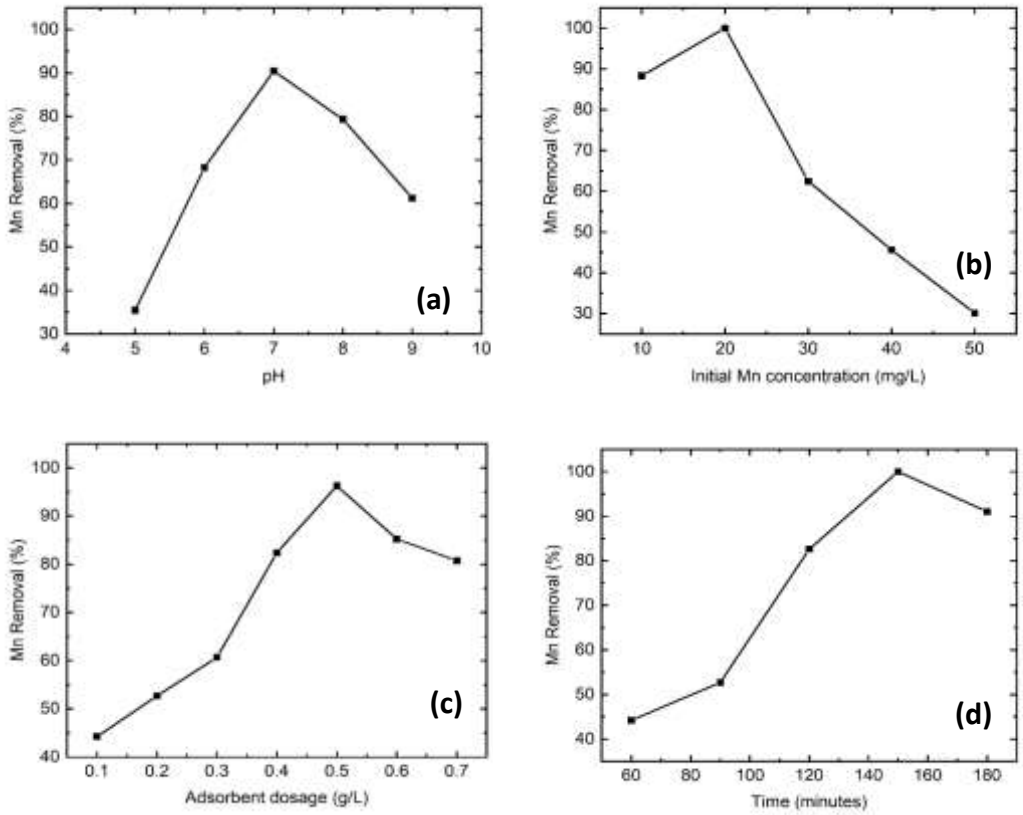

677 **Figure 7** Effect of (a) pH, (b) initial Mn concentration (mg/L), (c) BBP adsorbent dosage (g/L) and (d) contact
678 time (minutes) for Mn removal\

679

680

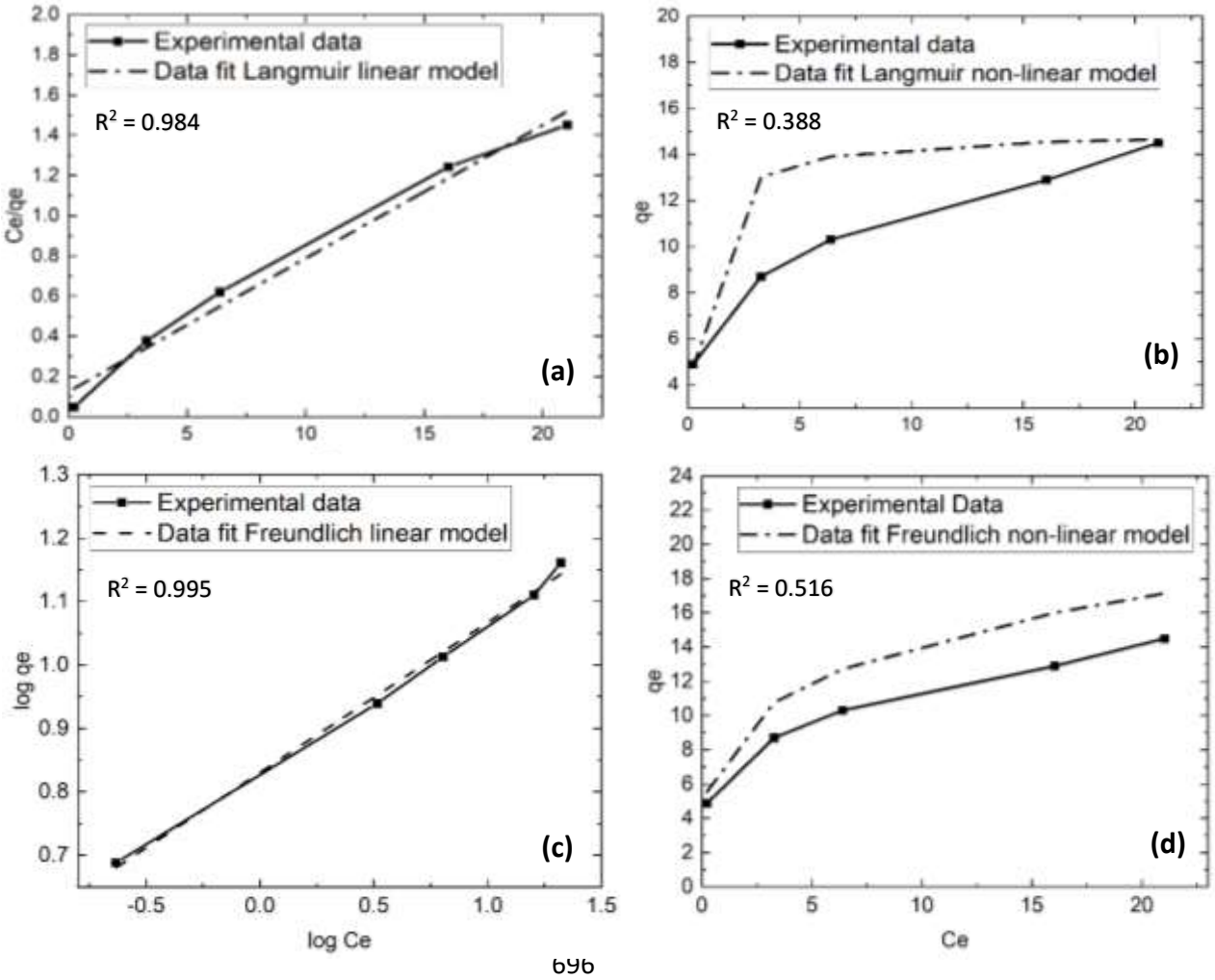

696

697 **Figure 8** (a) Linear and (b) non-linear of Langmuir isotherm; (c) Linear and (d) non-linear of Freundlich
698 isotherm model for Mn adsorption using BBP

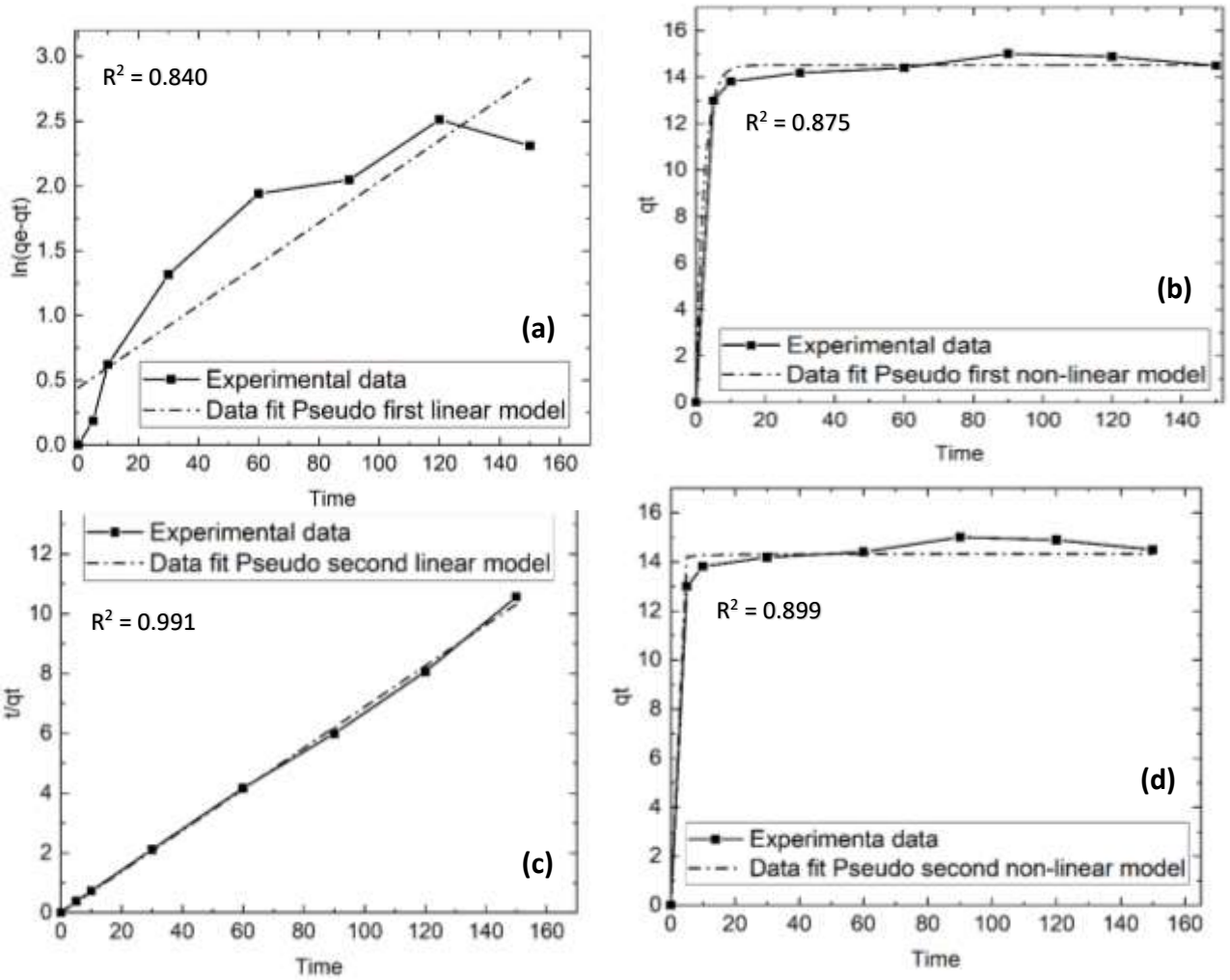

Figure 9 (a) Linear and (b) non-linear of Pseudo first order; (c) Linear and (d) non-linear of Pseudo second order kinetic model for Mn adsorption using BBP

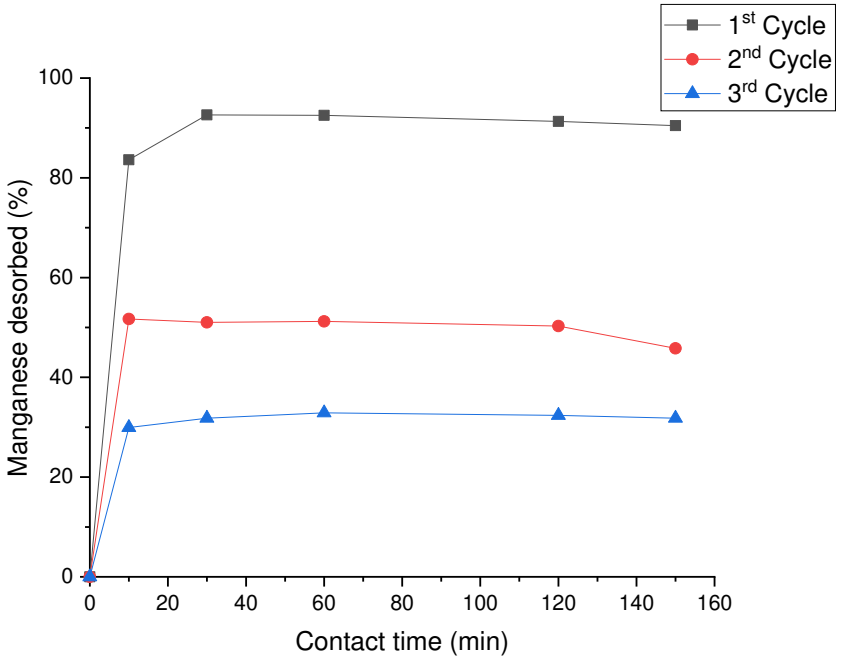

722

723 **Figure 10** Desorption of manganese by BBP adsorbent

724

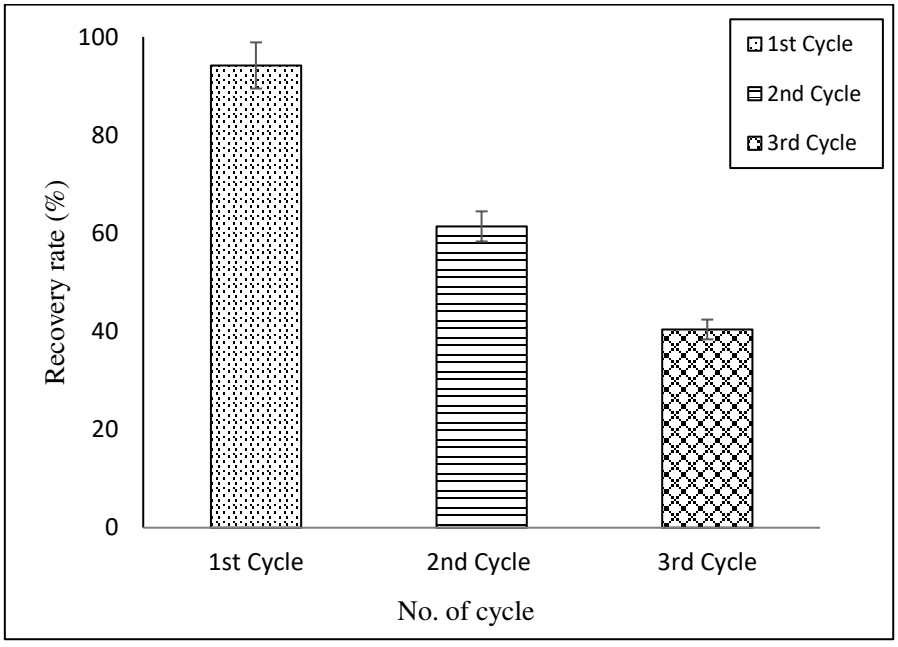

725

726 **Figure 11** Recovery of BBP adsorbent for manganese removal